trans-2-Phenylcyclopropylamine Is a Mechanism-Based Inactivator of the Histone Demethylase LSD1†

Dawn M. Z. Schmidt and Dewey G. McCafferty*

Department of Chemistry, B120 Levine Science Research Center, Box 90317, Duke University, Durham, North Carolina 27708

Received September 6, 2006; Revised Manuscript Received January 30, 2007

ABSTRACT: The catalytic domain of the flavin-dependent human histone demethylase lysine-specific demethylase 1 (LSD1) belongs to the family of amine oxidases including polyamine oxidase and monoamine oxidase (MAO). We previously assessed monoamine oxidase inhibitors (MAOIs) for their ability to inhibit the reaction catalyzed by LSD1 [Lee, M. G., et al. (2006) *Chem. Biol. 13*, 563−567], demonstrating that *trans*-2-phenylcyclopropylamine (2-PCPA, tranylcypromine, Parnate) was the most potent with respect to LSD1. Here we show that 2-PCPA is a time-dependent, mechanism-based irreversible inhibitor of LSD1 with a K_I of 242 μM and a k_{inact} of 0.0106 s^{-1}. 2-PCPA shows limited selectivity for human MAOs versus LSD1, with k_{inact}/K_I values only 16-fold and 2.4-fold higher for MAO B and MAO A, respectively. Profiles of LSD1 activity and inactivation by 2-PCPA as a function of pH are consistent with a mechanism of inactivation dependent upon enzyme catalysis. Mass spectrometry supports a role for FAD as the site of covalent modification by 2-PCPA. These results will provide a foundation for the design of cyclopropylamine-based inhibitors that are selective for LSD1 to probe its role in vivo.

Within eukaryotic cells, DNA is packaged into the higher order structure known as chromatin. The basic repeating unit of chromatin is the nucleosome, consisting of a histone octamer containing two copies each of histones H2A, H2B, H3, and H4, around which approximately 147 base pairs of DNA is wrapped. The histones of the histone octamer contain unstructured N-terminal "tails", the residues of which are the site of numerous posttranslational modifications, including acetylation of lysine, phosphorylation of serine and threonine, and methylation of lysine and arginine (*1*). Additionally, lysine residues may be mono-, di-, or trimethylated, while arginine residues may be mono- or dimethylated. The resulting complexity of modifications has been postulated to act as a "histone code", by which these patterns of modifications are "read" by the cellular machinery to produce a specific gene regulatory outcome (*2*, *3*).

For each histone modification, a complementary pair of enzymes exists to catalyze the addition and removal of these modifications as needed. Two classes of human enzymes capable of demethylating methylated lysine residues have been recently identified. JmjC domain-containing demethylases including JHDM3A/JMJD2A, GASC1/JMJD2C, JHDM2A, and JHDM1 comprise the first class (*4*−*8*); these enzymes appear to utilize the cofactors Fe(II) and α-ketoglutarate to demethylate via hydroxylation of the methyl group with subsequent elimination of formaldehyde. The second class of histone demethylases includes the amine oxidase domain-containing enzyme lysine-specific demethylase 1 (LSD1;[1] also referred to as BHC110) (*9*).

The amine oxidase domain of LSD1 is homologous to equivalent domains found in polyamine oxidase (PAO, 22.4% identity) and monoamine oxidases A and B (MAO A, 17.6% identity; MAO B, 17.6% identity). LSD1 catalysis is a flavin-dependent process in which formaldehyde and peroxide are produced as byproducts of histone demethylation (Figure 1) (*9*, *10*). The requirement for formation of positive charge on the ϵ-nitrogen atom of lysine in the imine intermediate limits LSD1 to demethylation of dimethylated and monomethylated lysine. This is in contrast to certain members of the JmjC domain-containing demethylases, which have been demonstrated to perform the demethylation of trimethylated lysine (*4*, *5*, *7*).

Because of the similarities between the catalytic sites of MAO A and B and LSD1, we previously assayed the ability of irreversible monoamine oxidase inhibitors (MAOIs, Table 1) to inhibit the function of LSD1 (*11*). MAOIs are well-known drugs that have been used clinically for the treatment of depression, anxiety, and Parkinson's disease (*12*). The majority of the molecules in Table 1 appear to exert their action through the irreversible modification of the covalently bound FAD, with varying selectivities for monoamine oxidase A (MAO A) and monoamine oxidase B (MAO B).

† This work was supported by Grant GM-65539 (to D.G.M.) from the National Institutes of Health. D.M.Z.S. was supported by an NRSA postdoctoral fellowship from the National Cancer Institute.

* To whom correspondence should be addressed. Telephone: (919) 660-1516. Fax: (919) 660-1605. E-mail: dewey@duke.edu.

[1] Abbreviations: LSD1, lysine-specific demethylase; MAO, monoamine oxidase; MAOI, monoamine oxidase inhibitor; 2-PCPA, *trans*-2-phenylcyclopropylamine; FAD, flavin adenine dinucleotide; HRP, horseradish peroxidase; 4-AAP, 4-aminoantipyrine; DCHBS, 3,5-dichloro-2-hydroxybenzenesulfonic acid; DMSO, dimethyl sulfoxide; TFA, trifluoroacetic acid; CHCA, α-cyano-4-hydroxycinnamic acid; MALDI-TOF, matrix-assisted laser desorption ionization−time of flight; MSOX, monomeric sarcosine oxidase; CPG, *N*-(cyclopropyl)glycine; SDS, sodium dodecyl sulfate; DNPH, dinitrophenylhydrazine; SET, single electron transfer.

10.1021/bi0618621 CCC: $37.00
Published on Web 03/17/2007

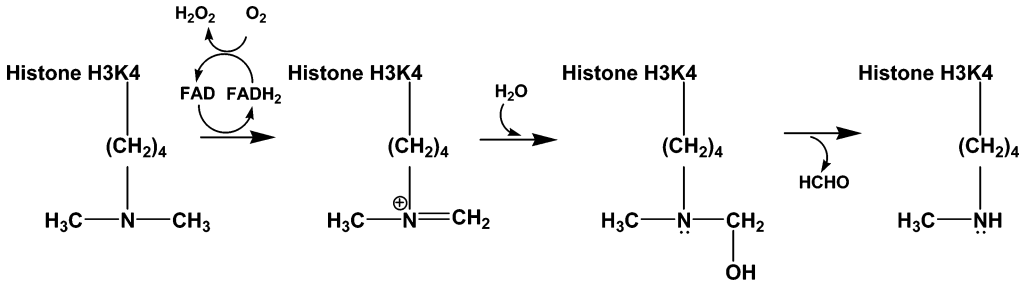

FIGURE 1: Proposed reaction scheme for demethylation of histone H3 methylated at Lys4.

Table 1: Irreversible Monoamine Oxidase Inhibitors

Inhibitor	Structure	Selectivity
2-PCPA	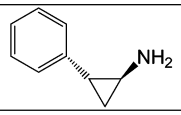	Nonselective
Nialamide	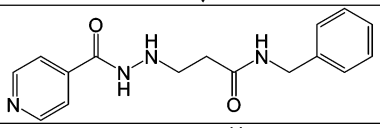	Nonselective
Phenelzine	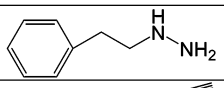	Nonselective
Deprenyl	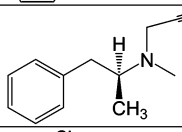	MAO B
Clorgyline	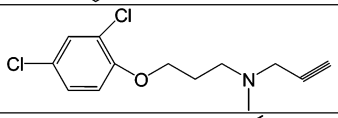	MAO A
Pargyline	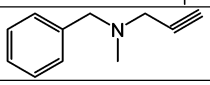	MAO B

LSD1 has been shown to possess a noncovalently bound FAD, similar to polyamine oxidases (*10*). Of the molecules shown, we demonstrated that *trans*-2-phenylcyclopropylamine (2-PCPA) displayed the highest apparent inhibitory potency and was also effective at inhibiting histone demethylation in vivo (*11*). 2-PCPA is a particularly interesting inhibitor of MAO, as attempts to identify the site of modification of MAO by 2-PCPA have been inconclusive. In this report, we further assess inhibition of LSD1 by MAOIs in a more quantitative fashion via kinetic analysis and seek to understand the mechanism of inhibition. The results presented here will provide a starting point for the design of more specific inhibitors of LSD1. LSD1 may also prove to be a more tractable system than MAOs for resolving long-standing uncertainties regarding the chemical mechanism of these flavin-dependent amine oxidases.

MATERIALS AND METHODS

Chemicals and Enzymes. Tyramine, horseradish peroxidase (HRP), 4-aminoantipyrine (4-AAP), and 3,5-dichloro-2-hydroxybenzenesulfonic acid (DCHBS) were purchased from Sigma. Amplex Red was obtained from Invitrogen. Fmoc-amino acids were from Novabiochem or Applied Biosystems. MAO A (150 units/mg) and MAO B (45 units/mg) were obtained as membrane preparations from Sigma and used without further purification. 2-PCPA hydrochloride was from BIOMOL Research Laboratories. Pargyline hydrochloride was obtained from Sigma.

Synthesis of Dimethylated H3 Peptide. A peptide corresponding to the first 21 amino acids of the N-terminal tail of histone H3, incorporating dimethylated lysine at residue 4 [ARTK(diMe)QTARKSTGGKAPRKQLA], was synthesized using standard Fmoc chemistry on an Applied Biosystems 433 peptide synthesizer using PAL resin (Advanced Chemtech). The C-terminal sequence GYG was added to allow for quantification of the peptide concentration at 280 nm, using an extinction coefficient of 1440 M^{-1} cm^{-1} for tyrosine (*13*). The peptide was purified using a reverse-phase C_{18} semipreparative column (Phenomenex), and its mass was verified by MALDI-MS (observed 2559.7, expected 2557.5).

Expression and Purification of LSD1. The construct described by Forneris and co-workers was used for expression and purification of LSD1 (*10*, *14*), with the exception that the gene encoding LSD1 was inserted into the vector pET151-D/TOPO (Invitrogen) instead of pET28b. The pET151-D/TOPO vector encodes an N-terminal six-histidine fusion tag with a TEV protease cleavage site. The final construct is missing the first 150 amino acids relative to the sequence reported by Shi et al. (*9*) but still contains the SWIRM and amino oxidase domains. This construct has previously been shown to be active toward peptide substrates in vitro (*10*, *14*).

BL21(DE3) *Escherichia coli* harboring the plasmid encoding LSD1 were grown at room temperature until reaching an OD_{600} of approximately 0.6, at which point protein expression was induced via the addition of 0.5 mM IPTG. The cells continued to grow overnight at room temperature before being harvested by centrifugation. Histidine-tagged LSD1 was purified and its concentration determined following published procedures (*14*). Glycerol was added to the final purified enzyme to a final concentration of 40% for storage at −20 °C; enzyme stored in this manner retained full activity for at least 3 months.

Assays for Lysine Demethylase and Monoamine Oxidase Inhibition by Monoamine Oxidase Inhibitors. Peroxide production by LSD1 or MAO was monitored using a HRP-coupled assay in 50 mM HEPES, pH 7.6. 4-AAP/3,5-DCHBS (0.1 mM/1.0 mM) was used as the chromogenic electron acceptor in absorbance-based assays, while Amplex Red (50 μM) was used as the fluorogenic electron acceptor in fluorescence-based assays. Final concentrations of 1 and 2 units/mL HRP were used to assay LSD1 and MAO, respectively. Absorbance assays were performed in a final volume of 50 μL in 96-well clear plate format and monitored at 510 nm in a Thermo Labsystems Multiskan Spectrum absorbance-based plate reader. Fluorescence assays were performed in a final volume of 60 μL in 96-well white plate format and monitored with 560 nm excitation and 590 nm

emission in a Molecular Devices SpectraMax Gemini EM plate reader. The linear range for each enzyme was determined (data not shown), resulting in the use of final concentrations of 0.5 μM LSD1, 7.8 units/mL MAO A, and 2.8 units/mL MAO B.

For assessment of inhibition of LSD1, the K_m^{app} for the dimethylated peptide substrate was first assayed and found to be 9.8 μM (data not shown). The use of K_m^{app} reflects the conversion of dimethylated substrate to unmethylated product via two demethylation events. This substrate concentration was then used in all subsequent inhibition assays. Similarly, the K_m values of MAO A and MAO B for tyramine were found to be 130 and 180 μM, respectively (data not shown), and these concentrations were used in subsequent inhibition assays as well.

MAOIs were prepared as 100 mM stocks in dimethyl sulfoxide (DMSO) and stored in aliquots at −20 °C. IC_{50} values were determined by preincubating the appropriate enzyme with varying concentrations of inhibitor for 15 min at room temperature prior to initiation of the reaction via the addition of substrate and coupling enzymes. In control experiments, DMSO was found to have no effect on enzyme activity at concentrations up to and including 10% (data not shown). The resulting data were converted to percent activity relative to a control reaction without inhibitor and fitted directly to eq 1 using the Grafit 4.0 software package (Erithacus Software):

$$\text{percent activity} = 100\{1/[1 + ([I]/IC_{50})^s]\} \quad (1)$$

where [I] is the inhibitor concentration and s is a slope factor.

To test for reversibility of inhibition of LSD1 by 2-PCPA, 50 μM enzyme was incubated with 200 μM 2-PCPA (10 × IC_{50}) or 0.2% DMSO as a positive control at 37 °C. Aliquots (0.5 μL) were removed at time points ranging from 15 to 150 min and used to initiate 50 μL reactions containing peptide substrate and coupling reagents (resulting in a dilution of inhibitor to a final concentration of 0.1 × IC_{50}) (*15*).

To determine rates of inactivation of LSD1 or MAO by 2-PCPA, reactions were initiated via addition of enzyme to assay solutions containing substrate and varying concentrations of inhibitor. The resulting progress curves were fit directly to eq 2 describing time-dependent inactivation (*15*) using GraFit to obtain values of k_{obs}:

$$\text{product} = (v_i/k_{obs})(1 - \exp^{-k_{obs}t}) \quad (2)$$

where v_i is the initial rate prior to inactivation, t is time, and k_{obs} is the observed rate of inactivation. The resulting values of k_{obs} were plotted as a function of inhibitor concentration to obtain values of K_I and k_{inact} according to eq 3 in GraFit (*15*):

$$k_{obs} = (k_{inact}[I])/(K_I + [I]) \quad (3)$$

where k_{inact} is the maximal rate of inactivation and K_I is the inhibitor concentration that yields half that rate of inactivation.

pH Profiles of LSD1 Activity and Inactivation by 2-PCPA. To examine the dependence of LSD1 activity and inactivation on pH, a series of buffers with overlapping pH values in 0.5 increments was used: MES (pH 6.5−7), HEPES (pH 7−8), TAPS (pH 8−9), CAPSO (pH 9−10), and CAPS (pH 10−11). The final concentration of each buffer in the assay was 50 mM; the final ionic strength was adjusted to 43.6 mM via the addition of the appropriate amount of concentrated NaCl. A full velocity versus substrate profile was determined in triplicate at each pH to obtain values of k_{cat} and k_{cat}/K_m. For the pH profile of inactivation, concentrations of 1000, 825, 650, 475, 300, and 125 μM 2-PCPA were used in duplicate with 9.8 μM substrate; however, only the three highest concentrations allowed reliable determinations of k_{obs} at all pH values. These concentrations of 2-PCPA correspond to the k_{inact} region of the k_{obs} vs [I] plot shown in Figure 4 and are therefore best compared to the profile for k_{cat}. Grafit v.4.0.21 (Erithacus Software) was used to fit pH profile data. For a profile exhibiting a double bell profile with an acidic limb slope of 1 and a basic limb slope of −1, the log values of the measured parameter were fit as a function of pH to the equation:

$$\log y = \log\{C/[1 + (H/K_1) + (K_2/H)]\} \quad (4)$$

where y is the measured parameter, C is the pH-independent value of y, H is the hydrogen ion concentration, and K_1 and K_2 are functional group acid dissociation constants (*16*). For profiles exhibiting a single ionization with an acidic limb slope of 1, the log values of the measured parameter were fit as a function of pH to the equation:

$$\log y = \log\{C/[1 + (H/K_1)]\} \quad (5)$$

where the meaning of all variables is identical to that in eq 4 above. LSD1 was stable at the extremes of the pH range tested (data not shown), indicating that the observed pH-dependent changes in activity were not due to instability of the enzyme.

Purification and Analysis of Flavin Intermediates from Inactivated LSD1. To isolate significant quantities of flavin intermediates from LSD1, large volumes of culture (11−30 L) were necessary, since a typical yield of purified LSD1 is <3 mg/L culture. LSD1 was purified as described above, except that no concentration of the enzyme was performed after the gel filtration chromatographic step (volume ∼50 mL). 2-PCPA (or an equivalent amount of DMSO as a control) was added to a final concentration of 500 μM and allowed to incubate with LSD1 overnight at room temperature. The inactivated enzyme was concentrated 10-fold and treated with 0.3% SDS on ice for 2.5 h. Free flavin intermediates were separated from denatured protein via passage through a 10000 MWCO centrifugal filter (Amicon). The filtrates were then loaded onto a C_{18} reverse-phase HPLC column and eluted with a profile of 2 min of water containing 0.1% trifluoroacetic acid (TFA) (buffer A), followed by a 30 min gradient of 0−30% buffer B (90% acetonitrile containing 0.1% TFA) at 1 mL/min. The column was maintained at 30 or 10 °C during the run through the use of a Peltier system. The elution profile was monitored at 254 nm, and the full absorbance spectrum of the eluate was also monitored to determine which peaks were to be collected. The eluted peaks were concentrated to dryness and resuspended in 200 μL of water. For analysis by matrix-assisted laser desorption ionization−time of flight (MALDI-TOF) mass spectrometry (PerSeptive Biosystems), 0.5 μL

samples were spotted on MALDI plates with 0.5 μL of α-cyano-4-hydroxycinnamic acid (CHCA) matrix (10 mg/mL). For analysis by electrospray ionization (ESI) mass spectrometry, flavin intermediates were analyzed by direct infusion on an Agilent 1100 Series LC/MSD Trap LC/MS system using the negative ion detection mode.

RESULTS AND DISCUSSION

Inhibition of LSD1 and MAOs by 2-PCPA and Pargyline. A Western blot based assay using crude histones or nucleosomes as substrates was previously employed to demonstrate 2-PCPA inhibition of LSD1 (*11*). To further characterize the inhibition of LSD1 by 2-PCPA in comparison with monoamine oxidases, we performed a series of experiments using a defined peptide substrate representing the N-terminal tail of histone H3 dimethylated at Lys4 and detecting subsequent hydrogen peroxide formation by LSD1 using horseradish peroxidase coupled to chromogenic or fluorogenic electron acceptor dyes. We determined values of 0.033 s^{-1}, 9.8 μM, and 3367 M^{-1} s^{-1} for k_{cat}^{app}, K_m^{app}, and k_{cat}/K_m^{app}, respectively. The use of apparent values reflects the use of a dimethylated substrate, which will undergo two demethylation events to become unmethylated product. These values are in good agreement with those reported previously for a similar substrate (*14*).

Dose−response experiments were performed in order to determine appropriate ranges of inhibitor concentrations to be used in subsequent experiments. These assays were initiated via addition of substrate (at a final concentration equal to its K_m) to enzyme that had been preincubated with inhibitor for 15 min as described in Materials and Methods. Using this method, we obtained IC_{50} values for 2-PCPA of 20.7 ± 2.1 μM for LSD1, 2.3 ± 0.2 μM for MAO A, and 0.95 ± 0.07 μM for MAO B. The lower apparent IC_{50} value of 2 μM previously reported for LSD1 in Western blot assays using bulk histones and nucleosomes as substrates can be attributed to the use of much lower effective concentrations of substrate. Additionally, as will be shown below, 2-PCPA is an irreversible inhibitor of LSD1, rendering IC_{50} determinations highly dependent on assay conditions and useful only as a reference point for further experiments.

Metzger and co-workers (*17*) have reported that the MAOI pargyline appears to inhibit LSD1-catalyzed demethylation of H3-Lys9 in the presence of the androgen receptor in a cell-based assay. Pargyline did not appear to inhibit LSD1 at concentrations up to 1 mM in this assay, in agreement with our previous Western blot analyses (*11*) and with other published results (*14*); significant inhibition was observed only at concentrations approaching 10 mM (data not shown). In contrast, pargyline inhibited MAO A and B with apparent IC_{50} values of 1.16 ± 0.04 and 0.19 ± 0.01 μM, respectively.

Changes in the Absorbance Spectrum of LSD1 upon Incubation with 2-PCPA. The noncovalent FAD cofactor of LSD1 exhibits a characteristic dual band absorbance spectrum, centered at 382 and 456 nm (Figure 2A). Upon incubation of LSD1 (32.2 μM) with 2-PCPA (100 μM), a series of changes occur to the flavin spectrum. The first is the formation of a third absorbance peak or shoulder at approximately 326 nm. The amplitude of this shoulder increases with time as LSD1 is incubated with 2-PCPA and is accompanied by a gradual decrease in the amplitudes of

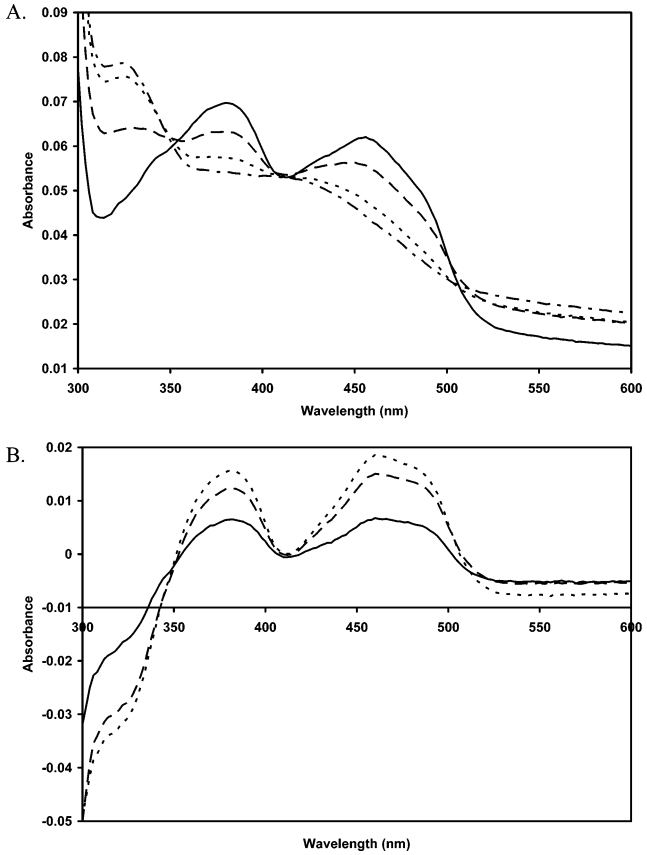

FIGURE 2: (A) Spectral changes upon incubation of 32.2 μM LSD1 with 100 μM 2-PCPA at 25 °C: solid line, immediately after mixing; dashed line, 5 min incubation; dotted line, 15 min incubation; dotted-dashed line, 60 min incubation. (B) Difference spectra (oxidized minus inhibited): solid line, 5 min incubation; dashed line, 15 min incubation; dotted line, 60 min incubation.

the peaks at 382 and 456 nm. These peaks are eventually resolved into a single absorbance peak at approximately 416 nm. These changes are further magnified in the difference spectra shown in Figure 2B. These changes are strikingly similar to those published by Singer's laboratory for beef liver MAO incubated with 2-PCPA (*18*). The similarities in the absorbance spectra of LSD1 and MAO in the presence of 2-PCPA may suggest a semblance in the intermediate formed.

The observed changes in the absorbance spectrum of LSD1 in the presence of 2-PCPA (Figure 2) are similar not only to that seen in bovine liver MAO exposed to 2-PCPA but also to those exhibited by the flavoprotein monomeric sarcosine oxidase (MSOX) when combined with the inhibitor *N*-(cyclopropyl)glycine (CPG) (*19*). MSOX utilizes a covalent FAD cofactor and catalyzes the oxidation of sarcosine (*N*-methylglycine) to glycine with the formation of formaldehyde and H_2O_2. In the presence of CPG under aerobic conditions, a charge-transfer complex is initially formed upon mixing, followed by the formation of a modified reduced flavin species with an absorbance maximum at 410 nm and a shoulder at 320 nm. The reduced flavin covalently modified by CPG at C(4a) has been predicted to undergo a retro-Michael addition to generate 1,5-dihydro-FAD, which can then be reoxidized to unmodified FAD by molecular oxygen (*20*). This mechanism would explain the observation that the level of inhibited MSOX reaches a steady-state level that is dependent upon CPG concentration; 11% of the enzyme is

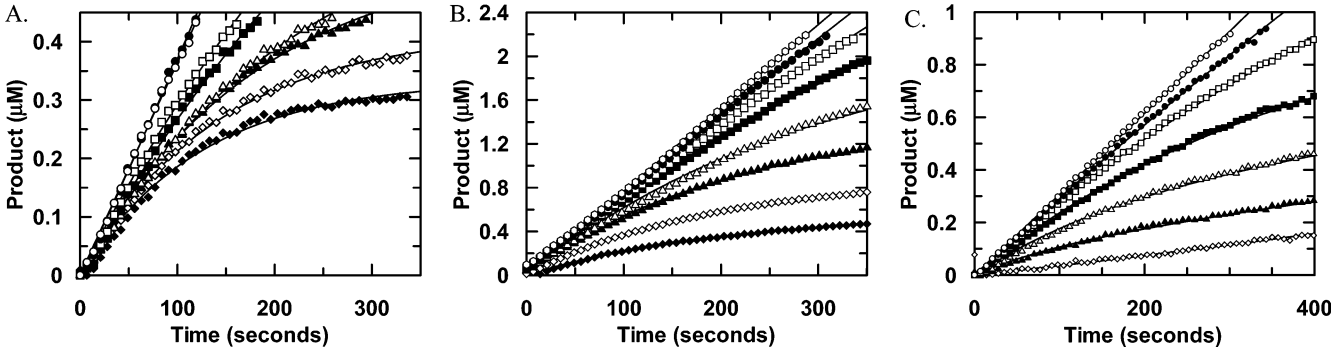

FIGURE 3: Representative progress curves for amine oxidase activity in the presence of varying concentrations of 2-PCPA. (A) LSD1 demethylation of a dimethylated Lys4-containing peptide in the presence of 750 μM (filled diamonds), 400 μM (open diamonds), 250 μM (filled triangles), 175 μM (open triangles), 100 μM (filled squares), 50 μM (open squares), 25 μM (filled circles), and 0 μM 2-PCPA (open circles). (B) MAO A deamination of tyramine in the presence of 500 μM (filled diamonds), 250 μM (open diamonds), 125 μM (filled triangles), 62.5 μM (open triangles), 31.3 μM (filled squares), 15.6 μM (open squares), 7.8 μM (filled circles), and 0 μM 2-PCPA (open circles). (C) MAO B deamination of tyramine in the presence of 100 μM (open diamonds), 25 μM (filled triangles), 12.5 μM (open triangles), 6.25 μM (filled squares), 3.13 μM (open squares), 1.56 μM (filled circles), and 0 μM 2-PCPA (open circles).

present as the oxidized charge-transfer complex even in the presence of a >15000-fold excess of CPG over enzyme (*19*).

Reversibility of 2-PCPA Inhibition of LSD1. 2-PCPA has long been known to act as an irreversible inhibitor of monoamine oxidases A and B (*18*, *21*). To determine whether 2-PCPA acts as an irreversible inhibitor of LSD1, we incubated 50 μM enzyme with 210 μM inhibitor at 37 °C. An equivalent amount of enzyme was incubated with 0.2% DMSO as a positive control. At time points ranging from 15 to 150 min, 0.5 μL aliquots were removed from both samples and diluted into assay solution containing substrate and coupling reagents with a final volume of 50 μL. This represents a 100-fold dilution that will reduce the inhibitor concentration in the assay to 0.1 × IC_{50}, which should yield 9% inhibition for a freely reversible enzyme inhibitor (*15*). 2-PCPA inhibition was irreversible within 60 min, with no recovery of demethylase activity upon dilution into the assay solution (data not shown).

To further confirm the irreversibility of 2-PCPA inhibition, 36.6 μM LSD1 was incubated with 550 μM 2-PCPA or 0.55% DMSO in a total volume of 100 μL overnight, followed by exhaustive dialysis against buffer (two changes of 4 L each). Absorbance scans taken before and after dialysis revealed no change in the spectra of either inactivated or active enzyme after dialysis, and no activity was recovered upon testing in the coupled assay (data not shown).

Inactivation Profiles of LSD1 and MAOs. In the presence of an irreversible inhibitor, progress curves of enzyme reactions initiated via addition of enzyme to assay solutions containing substrate and inhibitor will be nonlinear relative to assays without inhibitor (*15*), reflecting the time-dependent nature of the inhibition. The resulting progress curves can be fit to eq 2 as described in Materials and Methods to obtain values for k_{obs}, the rate of inactivation at each inhibitor concentration, which are then plotted as a function of inhibitor concentration as described in eq 3 to obtain values for k_{inact} and K_I. Representative progress curves for each enzyme are shown in Figure 3. Plots of k_{obs} versus inhibitor concentration were nonlinear, as expected for a mechanism-based irreversible inhibitor (Figure 4). The resulting values of k_{inact}, K_I, and k_{inact}/K_I are given in Table 2. Upon comparing values of k_{inact}/K_I for each enzyme, it is apparent that while 2-PCPA is most effective at inhibiting MAO B, it is not highly selective for this enzyme. The potency of inhibition by 2-PCPA of LSD1 and MAO A is similar and only about 7-fold less than that for inhibition of MAO B. The determined k_{inact}/K_I for MAO A is also in good agreement with a previously reported value for purified MAO A (*22*). Interestingly, the values for the maximal rate of inactivation, k_{inact}, are virtually identical within experimental error for all three enzymes, so that changes in k_{inact}/K_I are driven entirely by differences in the value of K_I. This suggests that there may be room for improving selectivity between LSD1 and MAO with cyclopropylamine as the bioactive pharmacophore. The k_{cat}/k_{inact} ratio is 3.1, indicating that inactivation occurs on a similar time scale as catalysis.

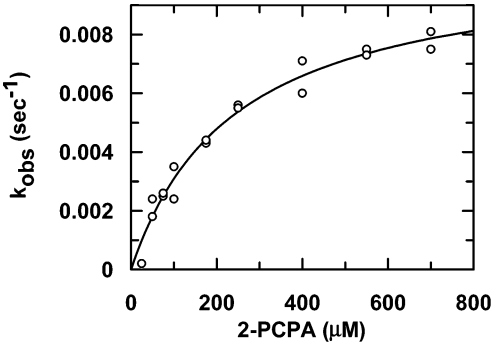

FIGURE 4: Rate of inactivation (k_{obs}) of LSD1 by 2-PCPA as a function of inhibitor concentration. Values of k_{obs} were determined from reaction progress curves as described in Materials and Methods.

Table 2: Kinetic Inactivation Parameters for Inhibition by 2-PCPA

enzyme	k_{inact} (s^{-1})	K_I (M)	k_{inact}/K_I (M^{-1} s^{-1})
LSD1	0.0106 ± 0.0006	242.7 ± 30.2	44 ± 6.0[a]
MAO A	0.0109 ± 0.0013	101.9 ± 39.5	107 ± 43.4[a]
MAO B	0.0113 ± 0.0023	16.0 ± 7.7	706 ± 368.9[a]

[a] Error shown is the propagated error from k_{inact} and K_I.

As noted above, pargyline appears to inhibit LSD1 activity at high concentrations. At 2.5, 5, and 10 mM pargyline, we were able to observe time-dependent inhibition of LSD1, yielding an apparent k_{inact}/K_I of 0.364 M^{-1} s^{-1}. Pargyline is therefore approximately 120-fold less potent than 2-PCPA toward LSD1.

pH Profiles of Inactivation of LSD1 by 2-PCPA. In order to determine if inactivation of LSD1 by 2-PCPA is dependent

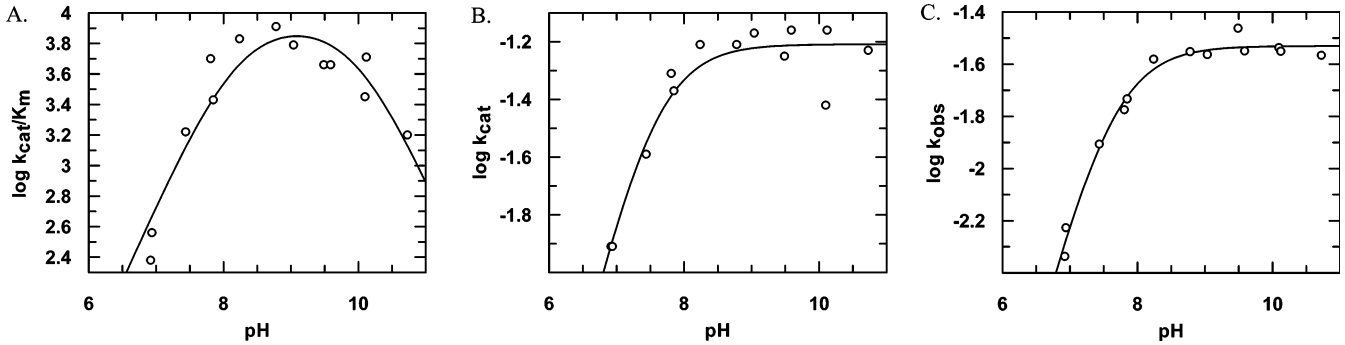

FIGURE 5: pH dependence of LSD1 activity. (A) log k_{cat} profile. (B) log k_{cat}/K_m profile. (C) log k_{obs} profile. Data shown are the average of triplicate measurements.

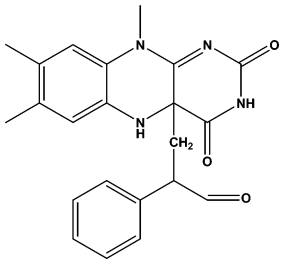

FIGURE 6: Proposed structure of the MAO B flavin cofactor covalently modified by 2-PCPA, from the structure in ref *23*.

upon enzyme catalysis, we compared the pH profiles for k_{cat} and k_{cat}/K_m with that for inactivation by 650 μM 2-PCPA, which is within the k_{inact} portion of the curve describing dependence of k_{obs} upon 2-PCPA concentration (Figure 4). The pH profile for log k_{cat} was best fit to a single acidic ionization with a slope of 1 (eq 4), yielding a pK_1 of 7.52 $\pm$ 0.07 (Figure 5A). The dependence of log k_{cat}/K_m on pH was described by a double bell ionization with slopes of 1 and -1 on the acidic and basic limbs, respectively (eq 5), giving pK_1 = 8.2 $\pm$ 0.3 and pK_2 = 10.1 $\pm$ 0.3 (Figure 5B).

The pH dependence of inactivation of LSD1 by 650 μM 2-PCPA was also fit to a single ionization profile with pK_1 = 7.60 $\pm$ 0.03 (Figure 5C). Identical profiles were obtained for the pH dependence of inactivation of LSD1 by 825 and 1000 μM 2-PCPA, but at lower concentrations of inhibitor values of k_{obs} could not be reliably determined at each pH (data not shown). The similarity of the pH profiles for k_{cat} and for inactivation strongly suggests that 2-PCPA is acting as a mechanism-based inactivator (*15*).

Investigating the Site of Modification of LSD1 by 2-PCPA. The apparent irreversibility of 2-PCPA inhibition of LSD1 suggests that covalent modification of the enzyme is likely as a mechanism of inhibition. Determining the site of modification is intriguing, because despite two decades of investigation, the site of modification of MAO (flavin or protein) by 2-PCPA has not been conclusively identified. Early biochemical work by Singer's laboratory and by Silverman (*18*, *21*) suggested that the enzyme, not the covalent flavin cofactor, was the site of modification. However, a structure of human mitochondrial monoamine oxidase B crystallized in the presence of 2-PCPA revealed that the inhibitor was bound to the flavin as a C(4a) adduct (Figure 6) (*23*), and a residue site of attachment to MAO has not yet been identified.

Because the FAD cofactor is noncovalently bound in LSD1, we were able to separate flavin from protein via

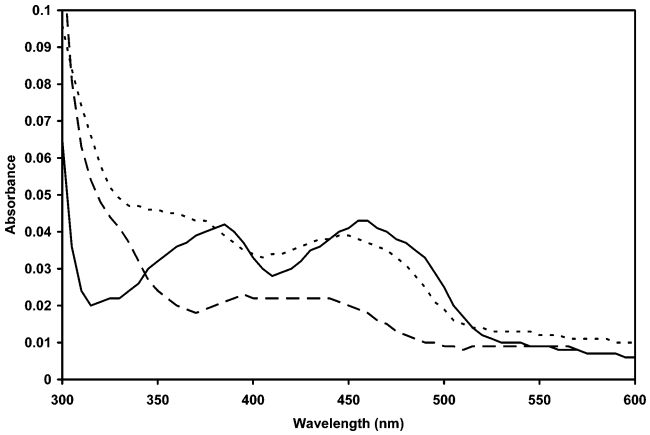

FIGURE 7: Instability of 2-PCPA-inactivated LSD1 to heat denaturation: solid line, 19.75 μM LSD1 prior to addition of 2-PCPA; dashed line, 19.75 μM LSD1 after inactivation with 200 μM 2-PCPA; dotted line, inactivated LSD1 after denaturation at 100 °C for 15 min followed by centrifugation to remove precipitated protein.

denaturation with 0.3% SDS, followed by purification by reverse-phase liquid chromatography. The reduced flavin intermediate of 2-PCPA-inactivated LSD1 is unstable to heat denaturation of LSD1, resulting in recovery of free oxidized flavin (Figure 7), but is relatively stable to the SDS denaturation procedure. In our initial experiments, chromatographic separation was performed with a C_{18} reverse-phase HPLC column maintained at 30 °C, and purified peaks were analyzed by MALDI-TOF mass spectrometry (Supporting Information). The elution profile was monitored at a single wavelength of 254 nm (corresponding to the nucleotide portion of FAD), as well as with a full absorbance scan between 190 and 900 nm to detect flavin species.

Flavin purified from LSD1 treated with 0.5% DMSO displayed only a single peak by HPLC corresponding to the expected mass for FAD (787 Da). Chromatographic analysis of flavin isolated from 2-PCPA-inactivated LSD1, followed by MALDI analysis of the collected peaks, revealed two flavin forms. The first, with a mass of 787 Da, corresponds to unmodified FAD, while the second gives a mass of 920 Da. This 920 Da species corresponds to an addition of 133 Da to FAD, which would give the expected mass for the FAD$-$2-PCPA adduct observed in the crystal structure of MAO B (Figure 6) (*23*). The absorption spectrum of the 920 Da species (Supporting Information) is also identical to that seen for 2-PCPA-inactivated LSD1 (Figure 2). The relative proportions of these two peaks with respect to the total flavin peak area were 55% and 45%, respectively.

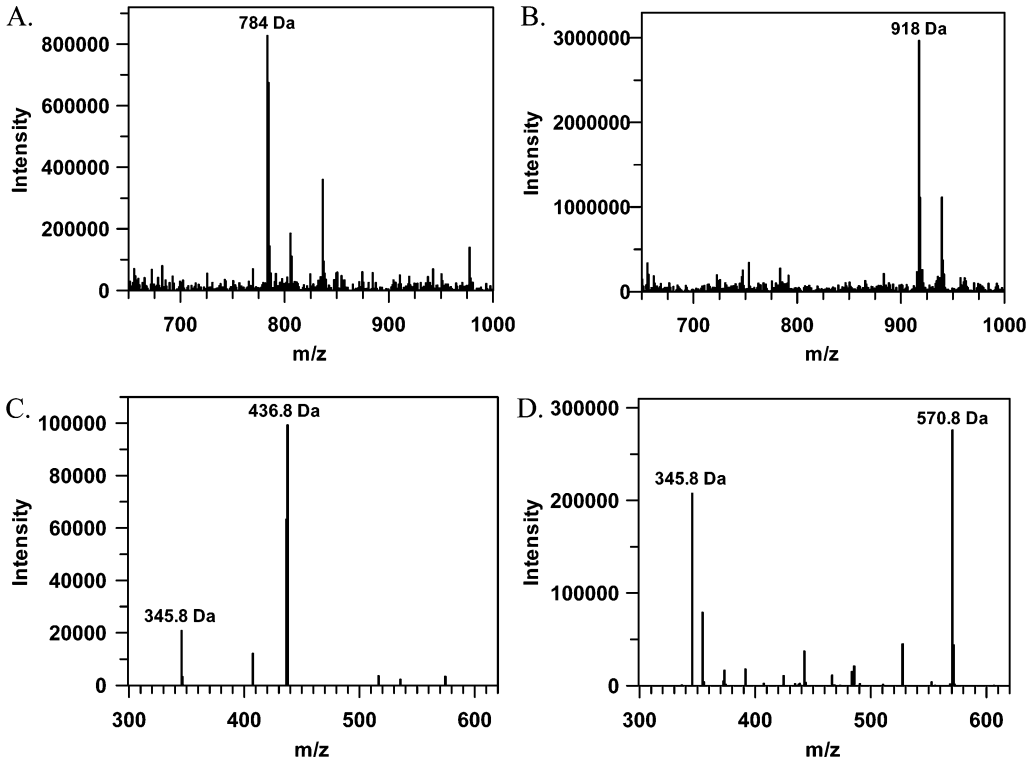

FIGURE 8: ESI-MS spectra of purified flavin species and fragmentation patterns. (A) Spectrum of unmodified FAD. (B) Spectrum of the 2-PCPA−FAD adduct. (C) Fragmentation pattern of the 784 Da molecular ion in the unmodified FAD spectrum. (D) Fragmentation pattern of the 918 Da molecular ion in the 2-PCPA−FAD adduct spectrum.

The previously observed sensitivity of the reduced flavin intermediate of 2-PCPA-inactivated LSD1 to heat denaturation led us to repeat our HPLC analysis with increased attention to temperature. By keeping the crude flavin mixture on ice and maintaining the HPLC column temperature at 10 °C, we were able to increase the proportion of the FAD−2-PCPA adduct with respect to the total flavin peak area to 83% (Supporting Information). This improvement in the purification procedure allowed us to isolate an increased amount of the proposed adduct for fragmentation analysis by electrospray ionization mass spectrometry (ESI-MS). Sodium borohydride treatment of 2-PCPA-inactivated LSD1 was ineffective at stabilizing the 2-PCPA−flavin adduct (data not shown).

Using the negative ion selection mode, unmodified flavin purified from denatured LSD1 yields a mass by ESI-MS of 784 Da (Figure 8). The proposed FAD−2-PCPA adduct gives a mass of 918 Da, again corresponding to the expected mass difference between the FAD−2-PCPA adduct observed in the crystal structure of MAO B and unmodified FAD. The molecular ion corresponding to 918 Da in the mass spectrum of the proposed 2-PCPA−flavin adduct was further fragmented to give ions with masses of 345.8 and 570.8 Da, while the molecular ion for FAD (784 Da) was fragmented to give ions with masses of 345.8 and 436.8 Da (Figure 8). For FAD, these ions correlate to that expected for AMP (345.8) and FMN (436.8). The difference in mass between the 436.8 Da ion fragment of FAD and the 570.8 Da ion fragment of the proposed 2-PCPA−flavin adduct, 134 Da, signifies that the site of attachment of 2-PCPA to the flavin is the isoalloxazine ring, as expected from the structure of MAO B (*23*).

In summary, our data demonstrate that 2-PCPA modifies FAD; the resulting modification is not susceptible to reduction by sodium borohydride and becomes unstable when the flavin adduct is removed from the active site environment of LSD1 through denaturation of the enzyme. Although we cannot conclusively rule out modification of an amino acid residue within the enzyme, our ability to recover up to 83% of the flavin cofactor as the 2-PCPA adduct from denatured, inactivated LSD1 indicates that FAD is likely the sole site of modification; recovery of 100% of the flavin cofactor as the adduct is limited by the apparent instability during sample handling as noted above. By analogy to the modification of FAD by CPG in MSOX (*19*) and by 2-PCPA in MAO B (*23*), we suggest that the point of attachment to the isoalloxazine ring in LSD1 may be C(4a).

CONCLUSIONS

The recently discovered histone demethylase LSD1 is subject to inhibition by the MAOI 2-PCPA, establishing that the activity of this enzyme can be effectively modified by a nonpeptidic small molecule. We have demonstrated here that this inhibition is irreversible and mechanism-based and presented evidence strongly suggesting that a covalent intermediate is formed between 2-PCPA and the noncovalent FAD cofactor of LSD1. Ultimate confirmation of the nature of the LSD1−2-PCPA adduct awaits further structural analysis. These data support using the reactive cyclopropylamine moiety as a building block in the design of inhibitors that will be selective for LSD1 versus MAOs.

Further investigation of the mechanism of LSD1 through the use of inhibitors could provide insight on the mechanism of MAO as well as identify differences between LSD1 and other amine oxidases. Two competing mechanisms have been proposed for MAO: the single electron transfer (SET) mechanism favored by Silverman (*24*) and the polar nucleo-

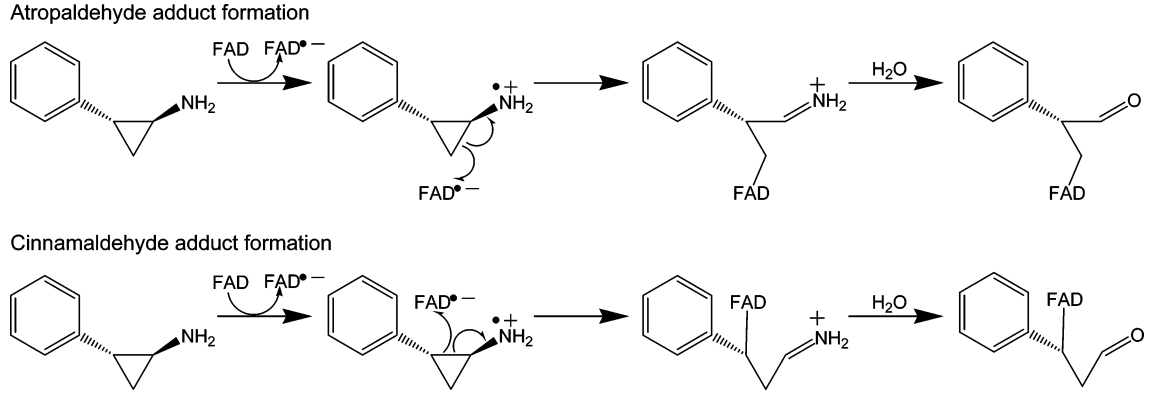

FIGURE 9: Possible mechanisms for modification of FAD by 2-PCPA in LSD1.

philic covalent mechanism proposed by Edmondson and coworkers (*25*). The attachment of 2-PCPA through a carbon−carbon bond at C(4a) is most consistent with a SET mechanism for MAO B and LSD1 (Figure 9). This intermediate is also similar to the proposed structure for the acyclic intermediate in the modification of FAD of MSOX at C(4a) by *N*-(cyclopropyl)glycine (*19*), which has also been postulated to proceed through a SET mechanism. Possible adducts between 2-PCPA and FAD resulting from a single electron transfer (SET) mechanism, depending on which carbon−carbon bond of the cyclopropyl ring is cleaved, include formation of a cinnamaldehyde adduct or an atropaldehyde adduct (Figure 9). Determining which bond is cleaved has important mechanistic implications; while cleavage of the bond leading to formation of the cinnamaldehyde adduct could proceed through formation of a benzylic radical not explicitly shown in Figure 9, formation of the atropaldehyde adduct would likely proceed through a concerted mechanism in which attack of the radical intermediate on the flavin precedes ring opening. We expect that the exact structure of the adduct formed between 2-PCPA and FAD should be the same for MAO B and LSD1, thereby corresponding to the atropaldehyde form. However, while fragmentation by ESI-MS of the isolated adduct clearly confirmed attachment to the isoalloxazine ring, no further diagnostic fragments were detectable. We are pursuing further strategies for stabilizing the 2-PCPA−FAD adduct for structural characterization, as well as the design of model compounds that may shed light on the structure of the adduct and reveal insights into the mechanism of LSD1.

It has previously been demonstrated that 2-PCPA is able to affect levels of histone H3K4 methylation in vivo in cell-based assays (*11*), and it is provocative to speculate whether amine oxidase homologues of MAO like LSD1 are targeted in the clinical use of MAOIs. It has been reported that high doses of 2-PCPA are effective in treating depression that is resistant to treatment, even though those doses were much larger than those reported to effect 90% MAO inhibition (*26*), indicating that 2-PCPA may be affecting more than MAO activity levels. Although 2-PCPA is the most potent of the MAOIs we have tested with respect to its ability to inhibit LSD1, it is intriguing that other MAOIs, including phenelzine, nialamide, and pargyline, are able to inhibit LSD1 as well (unpublished results and ref *11*). Further work, such as transcriptional analysis of cells exposed to MAOIs like 2-PCPA, will be required in order to establish a role for LSD1 inhibition in both the therapeutic and side effects of these drugs.

ACKNOWLEDGMENT

The authors thank an anonymous reviewer for helpful comments on the mechanism of adduct formation.

SUPPORTING INFORMATION AVAILABLE

HPLC chromatograms and MALDI-TOF spectra for the various purified FAD forms and the absorbance spectra of the purified FAD−2-PCPA adduct. This material is available free of charge via the Internet at http://pubs.acs.org.

REFERENCES

1. Zhang, Y., and Reinberg, D. (2001) Transcription regulation by histone methylation: interplay between different covalent modifications of the core histone tails, *Genes Dev. 15*, 2343−2360.
2. Cheung, P., Allis, C. D., and Sassone-Corsi, P. (2000) Signaling to chromatin through histone modifications, *Cell 103*, 263−271.
3. Strahl, B. D., and Allis, C. D. (2000) The language of covalent histone modifications, *Nature 403*, 41−45.
4. Cloos, P. A. C., Christensen, J., Agger, K., Maiolica, A., Rappsilber, J., Antal, T., Hansen, K. H., and Helin, K. (2006) The putative oncogene GASC1 demethylates tri- and dimethylated lysine 9 on histone H3, *Nature 442*, 307−311.
5. Klose, R. J., Yamane, K., Bae, Y., Zhang, D., Erdjument-Bromage, H., Tempst, P., Wong, J., and Zhang, Y. (2006) The transcriptional repressor JHDM3A demethylates trimethyl histone H3 lysine 9 and lysine 36, *Nature 442*, 312−316.
6. Tsukada, Y., Fang, J., Erdjument-Bromage, H., Warren, M. E., Borchers, C. H., Tempst, P., and Zhang, Y. (2006) Histone demethylation by a family of JmjC domain-containing proteins, *Nature 439*, 811−816.
7. Whetstine, J. R., Nottke, A., Lan, F., Huarte, M., Smolikov, S., Chen, Z., Spooner, E., Li, E., Zhang, G., Colaiacovo, M., and Shi, Y. (2006) Reversal of histone lysine trimethylation by the JMJD2 family of histone demethylases, *Cell 125*, 467−481.
8. Yamane, K., Toumazou, C., Tsukada, Y., Erdjument-Bromage, H., Tempst, P., Wong, J., and Zhang, Y. (2006) JHDM2A, a JmjC-containing H3K9 demethylase, facilitates transcription activation by androgen receptor, *Cell 125*, 483−495.
9. Shi, Y., Lan, F., Matson, C., Mulligan, P., Whetstine, J. R., Cole, P. A., Casero, R. A., and Shi, Y. (2004) Histone demethylation mediated by the nuclear amine oxidase homolog LSD1, *Cell 119*, 941−953.
10. Forneris, F., Binda, C., Vanoni, M. A., Mattevi, A., and Battaglioli, E. (2005) Histone demethylation catalysed by LSD1 is a flavin-dependent oxidative process, *FEBS Lett. 579*, 2203−2207.
11. Lee, M. G., Wynder, C., Schmidt, D. M., McCafferty, D. G., and Shiekhattar, R. (2006) Histone H3 lysine 4 demethylation is a target of nonselective antidepressive medications, *Chem. Biol. 13*, 563−567.

12. Riederer, P., Lachenmayer, L., and Laux, G. (2004) Clinical applications of mao-inhibitors, *Curr. Med. Chem. 11*, 2033−2043.
13. Byun, T., Tang, M., Sloma, A., Brown, K. M., Marumoto, C., Fujii, M., and Blinkovsky, A. M. (2001) Aminopeptidase from *Sphingomonas capsulata*, *J. Biol. Chem. 276*, 17902−17907.
14. Forneris, F., Binda, C., Vanoni, M. A., Battaglioli, E., and Mattevi, A. (2005) Human histone demethylase LSD1 reads the histone code, *J. Biol. Chem. 280*, 41360−41365.
15. Copeland, R. A. (2005) *Evaluation of Enzyme Inhibitors in Drug Discovery*, Wiley-Interscience, Hoboken, NJ.
16. Qian, J., West, A. H., and Cook, P. F. (2006) Acid-base chemical mechanism of homocitrate synthase from *Saccharomyces cerevisiae*, *Biochemistry 45*, 12136−43.
17. Metzger, E., Wissmann, M., Yin, N., Muller, J. M., Schneider, R., Peters, A. H., Gunther, T., Buettner, R., and Schule, R. (2005) LSD1 demethylates repressive histone marks to promote androgen-receptor-dependent transcription, *Nature 437*, 436−439.
18. Paech, C., Salach, J. I., and Singer, T. P. (1980) Suicide inactivation of monoamine oxidase by *trans*-phenylcyclopropylamine, *J. Biol. Chem. 255*, 2700−2704.
19. Chen, Z.-W., Zhao, G., Martinovic, S., Jorns, M. S., and Mathews, F. S. (2005) Structure of the sodium borohydride-reduced *N*-(cyclopropyl)glycine adduct of the flavoenzyme monomeric sarcosine oxidase, *Biochemistry 44*, 15444−15450.
20. Zhao, G., Qu, J., Davis, F. A., and Jorns, M. S. (2000) Inactivation of monomeric sarcosine oxidase by reaction with *N*-(cyclopropyl)-glycine, *Biochemistry 39*, 14341−14347.
21. Silverman, R. B. (1983) Mechanism of inactivation of monoamine oxidase by *trans*-2-phenylcyclopropylamine and the structure of the enzyme-inactivator adduct, *J. Biol. Chem. 258*, 14766−14769.
22. Vintem, A. P. B., Price, N. T., Silverman, R. B., and Ramsay, R. R. (2005) Mutation of surface cysteine 374 to alanine in monoamine oxidase a alters substrate turnover and inactivation by cyclopropylamines, *Bioorg. Med. Chem. 13*, 3487−3495.
23. Binda, C., Li, M., Hubalek, F., Restelli, N., Edmondson, D. E., and Mattevi, A. (2003) Insights into the mode of inhibition of human mitochondrial monoamine oxidase B from high-resolution crystal structures, *Proc. Natl. Acad. Sci. U.S.A. 100*, 9750−9755.
24. Silverman, R. B. (1995) Radical ideas about monoamine oxidase, *Acc. Chem. Res. 28*, 335−342.
25. Binda, C., Mattevi, A., and Edmondson, D. E. (2002) Structure-function relationships in flavoenzyme-dependent amine oxidations, *J. Biol. Chem. 277*, 23973−23976.
26. Baker, G. B., Coutts, R. T., McKenna, K. F., and Sherry-McKenna, R. L. (1992) Insights into the mechanisms of action of the MAO inhibitors phenelzine and tranylcypromine: a review, *J. Psychiat. Neurosci. 17*, 206−214.

BI0618621